Level Set-Based Topology Optimization for the Design of a Ferromagnetic Waveguide

doi: 10.1109/TMAG.2012.2196268

Level set-based topology optimization for the design of a ferromagnetic waveguide

Masaki Otomori[1], Takayuki Yamada[2], Kazuhiro Izui[1], Shinji Nishiwaki[1], and Nozomu Kogiso[3]

[1]Departmemt of Mechanical Engineering and Science, Kyoto University, Kyoto, Kyoto 606-8501, Japan
[2]Department of Mechanical Science and Engineering, Nagoya University, Nagoya, Aichi 464-8603, Japan
[3]Department of Aerospace Engineering, Osaka Prefecture University, Sakai, Osaka 599-8531, Japan

This paper discusses a level set-based topology optimization method for the design of a ferromagnetic waveguide. The optimization problem is formulated to maximize the power of transmitted waves at prescribed frequencies. A level set-based topology optimization method incorporating a fictitious interface energy is used to find optimized configurations of ferrite materials inside the waveguide. The results of the numerical examples for two different target frequencies show that the presented method successfully finds optimized configurations that maximize transmission power of waveguides for both forward and backward propagation.

Index Terms—**Ferromagnetic, waveguide, finite-element method, topology optimization, level-set method, left-handed materials.**

I. Introduction

Recent studies on the design of metallic waveguides with ferrite inclusions have generated increased interest in applying in microwave applications, such as waveguide filters and millimeter wave antennas [1], and also to the development of novel left-handed devices [2]. Ferrite materials exhibit a frequency-dependent value of permeability due to magnetic resonance phenomenon that can be altered by an externally applied DC magnetic field. Thus, metallic waveguides loaded with appropriately designed ferrite inclusions are expected to offer advantages such as tunable operating frequencies and compactness, because electromagnetic waves can propagate at frequencies below those of the cut-off frequency of the waveguide without the inclusions.

The topology optimization method [3] is the most flexible type of structural optimization method, and has been successfully applied in many design problems, including electromagnetic problems. For the design of metallic waveguides, Byun and Park [4] and Hirayama et al. [5] applied it to the design of dielectric inclusions inside a waveguide, Nishiwaki et al. [6] optimized the cross-sections of dielectric inclusions, and Yamasaki et al. [7] designed metallic inclusions for T-junctions and waveguide filters.

Here, a level set-based topology optimization method incorporating a fictitious interface energy [8] is used to find configurations of ferrite materials in a waveguide that maximize the transmission power of electromagnetic waves at prescribed frequencies. The Landau-Lifshitz model is used to express the permeability of the ferrite inclusions. The objective function is formulated to maximize the transmission coefficient S_{21} at prescribed desirable frequencies. The optimization algorithm uses the adjoint variable method (AVM) for the sensitivity analysis and the finite element method (FEM) for solving the equilibrium and adjoint equations, and updating the level set function. Numerical examples are provided to examine the validity and utility of the presented method.

Manuscript received March 2, 2012. Corresponding author: Masaki Otomori (e-mail: otomori.masaki.58r@st.kyoto-u.ac.jp).
Digital Object Identifier inserted by IEEE

II. Formulation

A. Ferrite materials

Ferrite materials exhibit a frequency-dependent permeability due to a magnetic resonance phenomenon, and the permeability can be altered by applying an external DC magnetic field. The magnetic permeability μ_f of a ferrite material can be described using the Landau-Lifshitz model, as follows.

$$\mu_f = \begin{bmatrix} \mu & \kappa j & 0 \\ -\kappa j & \mu & 0 \\ 0 & 0 & 1 \end{bmatrix}, \tag{1}$$

where

$$\mu = \frac{\omega^2 - \omega_0^2}{\omega^2 - \omega_h^2},\ \kappa = \frac{\omega\omega_m}{\omega^2 - \omega_h^2}. \tag{2}$$

In the above equations, ω is the angular frequency and ω_0 is the precession frequency. ω_0, ω_h and ω_m are defined as follows.

$$\omega_0 = \sqrt{\omega_h(\omega_h + \omega_m)}, \tag{3}$$

$$\omega_h = \gamma\mu_0\left(H_0 + j\frac{\Delta H}{2}\right), \tag{4}$$

$$\omega_m = \gamma\mu_0 M_S, \tag{5}$$

where γ and μ_0 are the gyromagnetic ratio of ferrite and the magnetic permeability of a vacuum, respectively. H_0, ΔH, and M_S are the magnitude of an externally applied DC magnetic field, the resonance line width of the ferrite material, and the degree of magnetization saturation, respectively.

B. 2D waveguide design problem

Here, we discuss the waveguide design problem. The design domain is illustrated in Fig.1. Transverse electric waves propagate in x-y direction where the electric field vector is polarized orthogonal to the direction of wave propagation. Incident waves enter the domain from the left boundary Γ_1, the upper and lower boundaries, Γ_{PEC}, are set as perfect electric conductors (PEC), and Γ_2 is output port. An external magnetic field is applied in the vertical (outward) direction

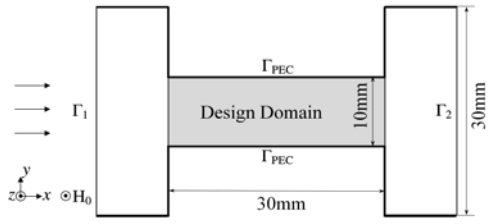

Fig 1. Design domain and boundary conditions.

perpendicular to the plane of the illustration. The governing equation is the 2-dimensional Helmholtz equation, which can be defined in weak form as follows:

$$a_1(E_z,\tilde{E}_z)+a_2(E_z,\tilde{E}_z)=l(\tilde{E}_z), \tag{6}$$

$$E_z=0 \quad \text{on} \quad \Gamma_{\text{PEC}}, \tag{7}$$

where

$$a_1(E_z,\tilde{E}_z)=\int_\Omega \nabla\tilde{E}_z\cdot\left(\mu_r^{-1}\nabla E_z\right)d\Omega-k_0^2\int_\Omega \varepsilon_r\tilde{E}_z E_z d\Omega, \tag{8}$$

$$a_2(E_z,\tilde{E}_z)=jk_0\int_{\Gamma_1\cup\Gamma_2}\sqrt{\varepsilon_r}\tilde{E}_z E_z d\Gamma, \tag{9}$$

$$l(\tilde{E}_z)=2jk_0\int_{\Gamma_1}\sqrt{\varepsilon_r}E_z^i\tilde{E}_z d\Gamma, \tag{10}$$

$$E_z\in U,\quad \forall\tilde{E}_z\in U, \tag{11}$$

$$U=\left\{\tilde{E}_z\in H^1(\Omega)\ \text{with}\ \tilde{E}_z=0\ \text{on}\ \Gamma_{\text{PEC}}\right\} \tag{12}$$

where E_z is the electric field, $\tilde{E}_z$ is the test function, E_z^i is the incident waves, μ_r and ε_r are the relative permeability and permittivity, respectively, k_0 is the wave number in a vacuum such that $k_0=\sqrt{\varepsilon_0\mu_0}$.

C. Level Set-Based Topology Optimization

Here, we briefly explain the level set-based topology optimization method that we apply [2]. Topology optimization is a method for optimizing material distribution in a fixed design domain D that consists of a solid domain Ω filled with solid material and a domain filled with void, with structural boundaries $\partial\Omega$.

In the level set-based method, the structural boundaries $\partial\Omega$ are expressed using the iso-surface of the level set function ϕ, as follows.

$$\begin{cases} 0<\phi(\mathbf{x})\le 1 & \text{if} \quad \forall\mathbf{x}\in\Omega\setminus\partial\Omega \\ \phi(\mathbf{x})=0 & \text{if} \quad \forall\mathbf{x}\in\partial\Omega \\ -1\le\phi(\mathbf{x})<0 & \text{if} \quad \forall\mathbf{x}\in D\setminus\Omega \end{cases}. \tag{13}$$

The optimization problem is then formulated as follows, using the level set-based boundary expressions defined above.

$$\inf_{\chi_\phi} \quad F(\chi_\phi)=\int_D f(\mathbf{x},\chi_\phi)d\Omega, \tag{14}$$

$$\text{s.t} \quad G(\chi_\phi)=\int_D g(\mathbf{x},\chi_\phi)d\Omega-G_{\max}\le 0, \tag{15}$$

where χ_ϕ is the characteristic function, f is the density function of the objective functional, g is the density function of the constraint functional, and $G_{\max}$ is the upper limit value of the constraint functional. The characteristic function χ_ϕ is defined as follows:

$$\chi_\phi(\phi)=\begin{cases}1 & \text{if} \quad \phi\ge 0\\ 0 & \text{if} \quad \phi<0\end{cases}. \tag{16}$$

The above formulation is an ill-posed problem because the level set function is allowed to be discontinuous at every point, so regularization must be applied. In the level set method used here, the Tikhonov regularization method is used. The above optimization problem is then replaced with the following optimization problem:

$$\inf_{\chi_\phi} \quad F_R(\chi_\phi,\phi)=F+R, \tag{17}$$

$$\text{s.t} \quad G(\chi_\phi)\le 0, \tag{18}$$

where R in the above equation is a regularization term defined as follows:

$$R=\int_D\frac{1}{2}\tau|\nabla\phi|^2 d\Omega, \tag{19}$$

where τ is a regularization parameter.

Next, the KKT conditions of the above optimization problem are derived as follows:

$$\left\langle\frac{d\overline{F}_R}{d\phi},\tilde{\phi}\right\rangle=0,\quad \lambda G=0,\quad \lambda\ge 0,\quad G\le 0, \tag{20}$$

where $\overline{F}_R=F_R+\lambda G$, $\overline{F}_R$ is the regularized Lagrangian, λ is the Lagrange multiplier, and $\left\langle d\overline{F}_R/d\phi,\tilde{\phi}\right\rangle$ represents the Fréchet derivative of the regularized Lagrangian $\overline{F}_R$ with respect to ϕ.

Although level set functions that satisfy the above KKT conditions are candidate solutions of the level set function that represents optimized configurations, it is not easy to find such solutions directly. Here, introducing a fictitious time t, we assume that the variation of the level set function is proportional to the gradient of Lagrangian $\overline{F}_R$, as follows:

$$\frac{\partial\phi}{\partial t}=-K(\phi)\frac{d\overline{F}_R}{d\phi}, \tag{21}$$

where $K(\phi)$ is a coefficient of proportionality.

Substituting Eq.(17) into Eq.(21), and setting an appropriate boundary condition, we have the following equations.

$$\begin{cases} \dfrac{\partial\phi}{\partial t}=-K(\phi)\left(\dfrac{d\overline{F}}{d\phi}-\tau\nabla^2\phi\right) & \\ \dfrac{\partial\phi}{\partial n}=0 & \text{on} \quad \partial D\setminus\partial D_N \\ \phi=0 & \text{on} \quad \partial D_N \end{cases}. \tag{22}$$

The optimization problem is then replaced by the above time evolutional equation. That is, optimal configurations can be obtained by solving the above time evolution problem.

D. Optimization Problem

The purpose of the optimization problem is to design a waveguide filter. The objective function is formulated to maximize the transmission power at frequency ω_i as follows:

$$\inf_{\Omega} \quad F=\sum_i\alpha_i\left|S_{21}\right|^2_{\omega=\omega_i}, \tag{23}$$

where α_i is a weighting function, S_{21} is the transmission coefficient of scattering parameters that can be obtained from the following equation.

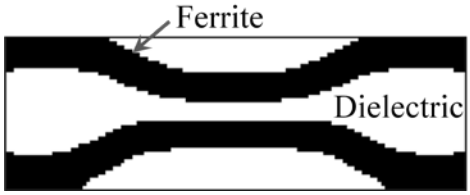

Fig 2. Optimized configuration of Example 1.

$$S_{21}(E_z)=\frac{\int_{\Gamma_2} E_z E_z^{i*}\,d\Gamma}{\int_{\Gamma_2} E_z^{i} E_z^{i*}\,d\Gamma}, \tag{24}$$

where E_z^{i*} indicates the conjugate of E_z^{i}.

E. Sensitivity Analysis

The sensitivity analysis is computed using the AVM. The Lagrangian of the optimization problem is formulated as follows:

$$\overline{F} = F + a(E_z, \tilde{E}_z) - l(\tilde{E}_z). \tag{25}$$

The sensitivity of the Lagrangian is obtained using the AVM as follows.

$$\begin{aligned}\left\langle \frac{\partial \overline{F}}{\partial \phi}, \tilde{\phi} \right\rangle &= \left\langle \frac{\partial F}{\partial S_{21}}, \tilde{S}_{21} \right\rangle \left\langle \frac{\partial S_{21}}{\partial E_z}, \tilde{E}_z \right\rangle \left\langle \frac{\partial E_z}{\partial \phi}, \tilde{\phi} \right\rangle \\ &\quad + \left\langle \frac{\partial a}{\partial E_z}, \tilde{E}_z \right\rangle \left\langle \frac{\partial E_z}{\partial \phi}, \tilde{\phi} \right\rangle + \left\langle \frac{\partial a}{\partial \phi}, \tilde{\phi} \right\rangle - \left\langle \frac{\partial l}{\partial \phi}, \tilde{\phi} \right\rangle \\ &= \left(\left\langle \frac{\partial F}{\partial S_{21}}, \tilde{S}_{21} \right\rangle \left\langle \frac{\partial S_{21}}{\partial E_z}, \tilde{E}_z \right\rangle + \left\langle \frac{\partial a}{\partial E_z}, \tilde{E}_z \right\rangle \right) \left\langle \frac{\partial S_{21}}{\partial \phi}, \tilde{\phi} \right\rangle \\ &\quad + \left\langle \frac{\partial a}{\partial \phi}, \tilde{\phi} \right\rangle - \left\langle \frac{\partial l}{\partial \phi}, \tilde{\phi} \right\rangle, \end{aligned} \tag{26}$$

where the adjoint variable is obtained by solving the following equation.

$$a(\delta E_z, \tilde{E}_z) = -\left\langle \frac{\partial F}{\partial S_{21}}, \tilde{S}_{21} \right\rangle S_{21}(\delta E_z), \quad \tilde{E}_z \in U, \forall\, \delta E_z \in U. \tag{27}$$

The sensitivity is finally obtained as follows.

$$\left\langle \frac{\partial \overline{F}}{\partial \phi}, \tilde{\phi} \right\rangle = \left\langle \frac{\partial a(E_z, \tilde{E}_z)}{\partial \phi}, \tilde{\phi} \right\rangle - \left\langle \frac{\partial l(\tilde{E}_z)}{\partial \phi}, \tilde{\phi} \right\rangle. \tag{28}$$

III. Numerical Examples

We now provide numerical examples of the 2D waveguide design problem. The design domain and boundary conditions are shown in Fig.1. The height and width of the waveguide are set to 10 mm and 30 mm, respectively. Incident waves enter the domain from the left, and the upper and lower boundaries are set as having the condition of a perfect electric conductor (PEC). Input and output ports are placed on the left and right sides of the design domain, to numerically support the TE_{10} mode. The entire domain is discretized using 14,440 rectangular elements. For the following examples, the conceptual material has parameters set as follows: $\gamma = 1.759 \times 10^{11}$, $\mu_0 H_0 = 30\text{mT}$, $\Delta H = 1\text{mT}$, and $\mu_0 M_0 = 173\text{ mT}$, assuming that the ferrite material resembles a yttrium iron garnet. The relative permittivity constant of the ferrite material, ε_r, is set to 10-1j. We also assume that the dielectric material used as the background material has the same relative permittivity constant as the ferrite material. A configuration filled with ferrite materials is used as initial configuration for both cases.

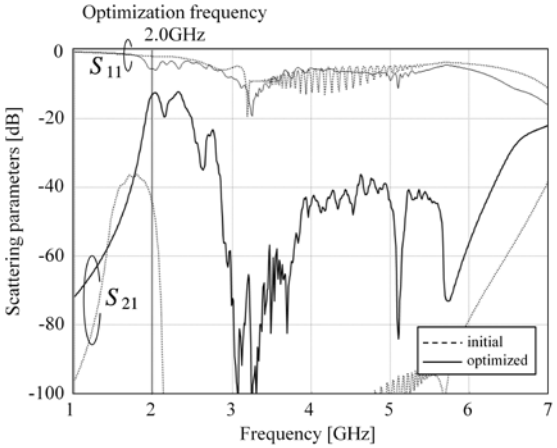

Fig 3. Frequency characteristics of scattering parameters S_{11} and S_{21} of Example 1, maximizing S_{21} at 2.0 GHz

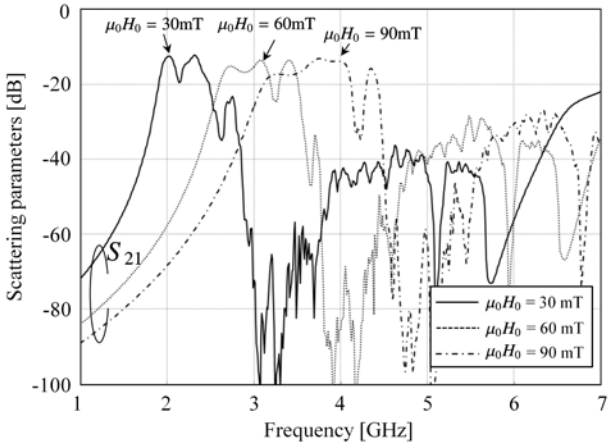

Fig 4. Frequency characteristics of scattering parameter S_{21} obtained using the optimized configuration of Example 1, with $\mu_0 H_0$ = 30mT, 60 mT and 90 mT, respectively.

A. Example 1: maximizing transmission power at 2.0 GHz

Figure 2 shows the optimized configuration, maximizing S_{21} at 2.0 GHz. Only the optimized configuration in the design domain is shown. The asymmetry in the optimized configuration is caused by the anisotropy of the ferrite material's permeability. Figure 3 shows the frequency characteristics of the scattering parameters S_{11} and S_{21} as the transmission coefficient S_{21} is increased over a broad frequency range. The transmission coefficient S_{21} is increased to roughly -12 dB at 2.0 GHz.

Figure 7(a) shows the electric field at 2.0 GHz for different phases of incident waves, namely, (i) 0°, (ii) 60°, (iii) 120°, and (iv) 180°. These figures show forward wave propagations in the waveguide. As the optimization results show, the optimized configuration consists of two bars located in the upper and lower areas of the design domain. Electromagnetic waves propagate in the dielectric material between the upper and lower ferrite bars that guide the transmission of electromagnetic waves. Figure 4 shows the frequency

Fig 5. Optimized configuration of Example 2.

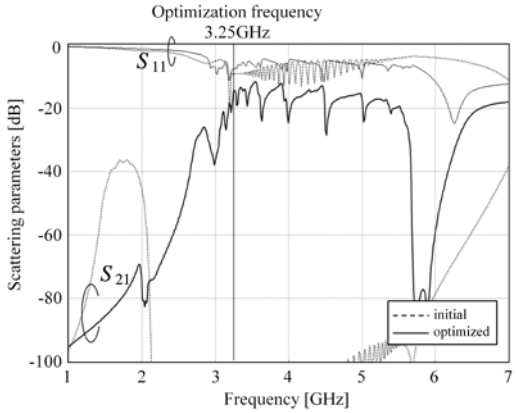

Fig 6. Frequency characteristic of scattering parameters S_{11} and S_{21} of Example 2, maximizing S_{21} at 3.25 GHz

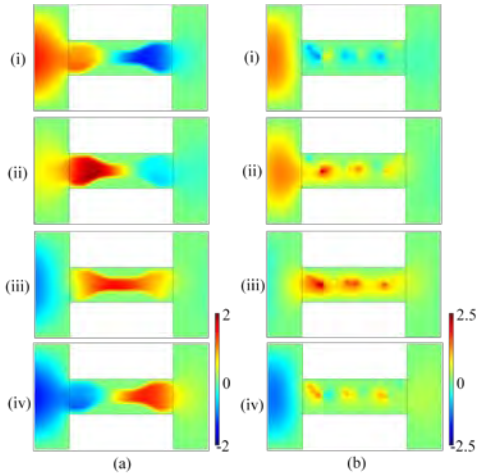

Fig 7. Electric fields of optimized configuration: (a) Example 1 at 2.0 GHz: (b) Example 2 at 3.25 GHz for various phases of incident waves: (i) 0°; (ii) 60°; (iii) 120°; (iv) 180°.

characteristics of the scattering parameters S_{21} for the obtained optimized configuration when different magnitudes of an external magnetic field are applied, with $\mu_0 H_0$ = 30 mT, 60 mT, and 90 mT, respectively. These illustrate the tunability of the operating frequency by the application of externally magnetic fields.

B. Example 2: maximizing transmission power at 3.25 GHz

Figure 5 shows the optimized configuration when S_{21} is maximized at 3.25 GHz. Figure 6 shows the frequency characteristics of the scattering parameters S_{11} and S_{21}, as the transmission coefficient S_{21} is increased to roughly -14 dB at 3.25 GHz.

Figure 7(b) shows the electric field at 3.25 GHz at different phases of incident waves. In contrast to the results of Example 1, the optimized configuration consists of a single ferrite bar, and the electromagnetic waves are strongly excited at the

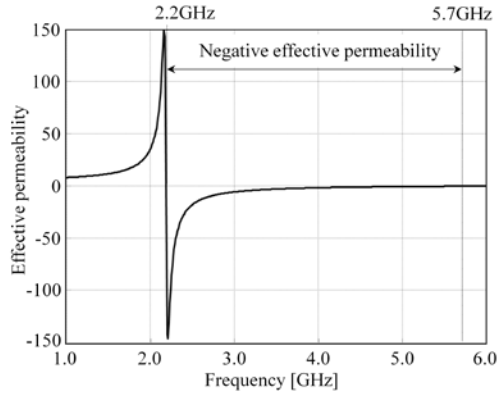

Fig 8. Effective permeability curve of the ferrite material.

horizontal interface between the ferrite and dielectric materials. This phenomenon resembles the edge guide mode of a ferrite-metallic plate system. Although the figures do not provide a clear indication, backward waves propagate in the waveguide due to the left-handed behavior of the waveguide. We note that in rectangular metallic waveguides, the effective dielectric constant becomes negative at frequencies below the cut-off frequency. Figure 8 shows the effective permeability of the ferrite material obtained by following equation.

$$\mu_{eff} = \frac{\omega^2 - (\omega_m + \omega_h)^2}{\omega^2 - \omega_0^2}, \tag{29}$$

The effective permeability also becomes negative at 3.25 GHz, so the waveguide exhibits left-handed behavior.

IV. Conclusion

In this study, a level set-based topology optimization method incorporating a fictitious interface energy was applied to the design of ferrite inclusions in a waveguide. The objective function was formulated to maximize the transmission power. The numerical examples for two different target frequencies show that the optimization method successfully found configurations that maximize the transmission power of waveguides for both forward and backward propagation.

Acknowledgment

This work was partially supported by the JSPS, Grant-in-Aid for Scientific Research (B), 22360041. The first author is partially supported by AISIN AW CO., LTD. We sincerely appreciate this assistance.

References

[1] K. C. Hwang and H. J. Eom, “Radiation from a ferrite-filled rectangular waveguide with multiple slits,” *IEEE Trans. Magn.*, vol.15, no. 5, pp. 345-347, 2005.

[2] T. Ueda and M. Tsutsumi, “Left-handed transmission characteristics of rectangular waveguides periodically loaded with ferrite,” *IEEE Trans. Magn.*, vol. 41. no. 10, pp. 3532-3537, October 2005.

[3] M. P. Bendsøe and N. Kikuchi, “Generating optimal topologies in structural design using a homogenization method,” *Comput. Methods Appl. Mech. Engrg.*, vol. 71, pp. 197-224, Nov. 1988.

[4] J. K. Byun and I. H. Park, “Design of dielectric waveguide filters using topology optimization technique,” *IEEE Trans. Magn.*, vol. 43. no. 4, pp. 1573-1576, April 2007.

[5] K. Hirayama, Y. Tsuji, S. Yamasaki and S. Nishiwaki, “Design optimization of H-plane waveguide component by level set method,” IEICE Trans. Electron., vol. E94-C, no. 5, May 2011.
[6] S. Nishiwaki, T. Nomura, S. Kinoshita, K. Izui, M. Yoshimura, K Sato and K. Hirayama, “Topology optimization for cross-section design s of electromagnetic waveguides targeting guiding characteristics,” *Finite. Elem. Anal.*, vol. 45, no. 12, pp. 944-957, 2009.
[7] S. Yamasaki, T. Nomura, A. Kawamoto, K. Sato and S. Nishiwaki, “A level set-based topology optimization method targeting metallic waveguide design problems,” *Int. J. Numer. Meth. Engng.*, vol. 87, no. 9, pp. 844-868, 2011.
[8] T. Yamada, K. Izui, S. Nishiwaki and A. Takezawa, “A topology optimization method based on the level set method incorporating a fictitious interface energy,” *Comput. Method Appl. M.*, vol. 199, no. 45-48, pp. 2876-2891, 2010.